P1.27 A NUMERICAL STUDY OF NEAR-FIELD DISPERSION WITHIN AND ABOVE FOREST CANOPIES

Edburg S.*, Stock D.[1], Lamb B.[1], Thistle H.[2]
[1]Washington State University, Pullman, WA
[2] U.S.D.A. Forest Service, Morgantown, WV

1. ABSTRACT

Pheromone releases are used by forest managers as an anti-aggregation technique to protect high value forest stands against the bark beetle. As a result, near-field pheromone dispersion patterns are of interest for developing forest management techniques. Recent field experiments have studied the dispersion of a tracer gas released from a point source in several different types of forest canopies. The objective of this paper is to investigate the feasibility of simulating turbulent transport within a forest canopy using a commercial Computational Fluid Dynamics (CFD) code. As a first step, Fluent was used to predict near-field concentrations of a tracer gas in a Lodgepole Pine canopy. A porous media based on the Leaf Area Index (LAI) and stem density measurements was used to simulate the effects of the canopy. Solar radiation effects on the canopy and ground were used to account for the development of a convective boundary layer above the canopy. Normalized concentrations for different downstream distances are presented as a basis for evaluation of the model performance.

2. INTRODUCTION

Mountain Pine Beetle (MPB) and the Southern Pine Beetle (SPB) infestations have dramatically increased over the past several years due to ecological factors including drought, age, and canopy density. This has directly impacted recreational use, wildlife habitat and silvicultural practice. In one case, the U.S.D.A Forest Service reported a 70 percent reduction of the red-cockaded woodpecker habitat in the Daniel Boone National Forest located in southern Kentucky. It has also been reported that 34,000 acres of lodgepole pine in Colorado is at moderate to high risk of MPB infestation. The U.S.D.A Forest Service has implemented many plans to control the Bark Beetle (U.S.D.A. Forest Service 2003).

Bark Beetles use a sophisticated pheromone system to communicate. Part of this communication system includes an anti-aggregation pheromone used to prevent overpopulation of host trees and promote the attack of other trees.

* *Corresponding author address*: Steven L. Edburg, Washington State University, School of Mechanical and Materials Engineering, Pullman WA 99164-2920; e-mail: sedburg@mail.wsu.edu

Forest managers are currently applying anti-aggregation management techniques as a control strategy. Present management techniques include deploying permeable packets from which an anti-aggregation pheromone diffuses into the surrounding canopy. However, there is little information available to guide the managers in effective placement of the packets (Thistle et al. In Press)

Several field studies have been conducted to gain insight into tracer gas dispersion within forest canopies. The studies have shown a strong link between tracer gas dispersion and meteorology and canopy density. However field studies are limited due to cost, location, meteorological conditions, etc. Numerical studies are less expensive and allow for many variations which are not feasible in field studies. This study investigates the feasibility of using computational fluid dynamics, CFD, to predict dispersion within a forest canopy.

Analytical models such as Gaussian models and numerical models based on gradient transport theory can be used when faced with uniform flows and homogenous turbulence. However, certain atmospheric parameters must be specified by the user, such as eddy diffusivities. These models work well in cases of homogenous

turbulence over uniform terrain, although for complex terrain first and second order turbulence closure models are better suited (Arya 1999). Flow and dispersion within forest canopies is highly stochastic spatially and temporal. Numerical models must be able to capture the three dimensionality of the turbulence in order to predict reasonable concentration fields. CFD has the capability to predict non-homogenous turbulence fields within complex geometries, at a high resolution.

As a first step, a numerical simulation has been used to study dispersion in a generic lodgepole pine forest canopy based on leaf area index (LAI) and stem density. The work described in this paper addresses the dispersion of a tracer gas within the canopy with and without solar heating.

3. EXPERIMENTAL STUDIES

Field Campaigns

Recent field studies have provided some insight into pheromone dispersion within forest canopies. Four canopies have been studied; two ponderosa pine canopies, an oak hickory canopy, and a lodgepole pine canopy. In each canopy downstream concentrations were collected along with corresponding meteorological data.

An array of syringe samplers were positioned on 5m, 10m, and 30m radial arcs from the release source and 1.5m above the ground. These samplers collected thirty minute averages of tracer gas concentration. Sulfur Hexafluoride, SF_6, was used as the tracer gas, and released at known rates from a point source, at the center point of the arcs. Three-axis sonic anemometers were used to gather meteorological data; these were positioned at the source, and on a tower at heights of 2.5m, 15m and 25.2m. Two levels of wind speed and direction, humidity, temperature, and net radiation were also collected using two 7m high meteorological towers. One sided LAI was also collected at each site.

4. COMPUTATIONAL MODEL

Governing Equations

The governing equations are based on conservation principles. Conservation of mass, momentum, energy, and species mass fraction are listed below.

Conservation of Mass

The continuity equation is

$$\frac{\partial \rho}{\partial t} + \frac{\partial}{\partial x_i}\left(\rho \overline{u}_i\right) = 0\,, \qquad (1)$$

where ρ is the density, and $\overline{u}_i$ is the velocity.

Conservation of Momentum

The time averaged conservation of momentum can be written as

$$\frac{\partial}{\partial t}\left(\rho \overline{u}_i\right) + \frac{\partial}{\partial x_j}\left(\rho \overline{u}_i \overline{u}_j\right) = -\frac{\partial \overline{p}}{\partial x_i} + \frac{\partial}{\partial x_j}\left[\mu\left(\frac{\partial \overline{u}_i}{\partial x_j} + \frac{\partial \overline{u}_j}{\partial x_i} - \frac{2}{3}\delta_{ij}\frac{\partial \overline{u}_i}{\partial x_i}\right)\right] + \frac{\partial}{\partial x_j}\left(-\rho \overline{u_i' u_j'}\right) - \delta_{i3}\,\rho g + S_i\,, \qquad (2)$$

where p is the pressure, μ is the dynamic viscosity, δ_{ij} is the Kronecker delta, $\overline{u_i' u_j'}$ are the Reynolds stresses, g is the gravity assumed to be in the negative z direction, and S_i is a momentum source term.

Conservation of Energy

The time averaged energy equation has the following form:

$$\frac{\partial}{\partial t}(\rho E)+\frac{\partial}{\partial x_i}\left[\overline{u}_i(\rho E+p)\right]= \frac{\partial}{\partial x_j}\left[\left(k+\frac{c_p\mu_t}{\mathrm{Pr}_t}\right)\frac{\partial\overline{\theta}}{\partial x_j}\right]+S_h \quad (3)$$

E is the total energy, k is the thermal conductivity, c_p is the specific heat, μ_t is the turbulent viscosity, Pr_t is the turbulent Prandtl number, set at 0.85, θ is the potential temperature, and S_h is a source term. The turbulent viscosity was modeled as

$$\mu_t=\rho C_\mu\frac{k^2}{\varepsilon}, \quad (4)$$

where C_μ = 0.09, k is the turbulent kinetic energy, and ε is the turbulent dissipation rate.

Conservation of Species Mass Fraction

The time averaged convection-diffusion conservation equation, for a species i , is

$$\frac{\partial}{\partial t}(\rho Y_i)+\frac{\partial}{\partial x_j}(\rho\overline{u}_j Y_i)= -\frac{\partial}{\partial x_i}(J_i)+R_i+S_i \quad , \quad (5)$$

where S_i is a source term, R_i is a reaction term, J_i is a diffusion term, and Y_i is the local mass fraction. For turbulent flows the mass diffusion is defined as

$$J_i=-\left(\rho D_{i,m}+\frac{\mu_t}{Sc_t}\right)\frac{\partial}{\partial x_i}Y_i, \quad (6)$$

where $D_{i,m}$ is the molecular diffusion coefficient for species i, and the turbulent Schmidt number, Sc_t, was set at 0.7.

Turbulence Model

Turbulent transport in forest canopies is dominated by turbulent eddies varying with time and space. Since time averaged equations were used, we need only to model the spatial variation of turbulence. First order models, such as the k-ε turbulence closure model, set dispersion coefficients in all directions proportional to the vertical momentum flux, thus lateral dispersion is inherently wrong. Furthermore transport from large convective eddies is not accounted for. Second order models, such as the Reynolds stress model (RSM), solve the momentum fluxes in all directions directly, capturing the lateral dispersion, and convective eddies. The RSM closure used in this study, followed Launder et al. (1975), however, the heat and species fluxes, $\overline{u_i'\theta'}$ and $\overline{u_i'Y'}$ respectively, were not directly solved, these were calculated using first order equations in Equation 3 and Equation 5 respectively.

Canopy Representation

A generic Lodgepole pine canopy was modeled as a horizontal homogenous porous media. Forest canopies are typically spatially inhomogeneous, but lodgepole pine canopies are relatively homogeneous in the horizontal. Porous media was used to simulate the canopy and provide the sink for momentum. The physical geometry is not represented in this approach, instead inertial loss terms are calculated to provide the same net effect on the flow. Inertial loss terms, as a function of height, were calculated from a LAI of 2.1 and a stem density of 1521 stems/hectare.

Momentum sinks based on LAI per unit volume, α_z, have been well documented by Raupach and Thom (1981); Amiro (1990); Kaimal and Finnigan (1994), and have the following form:

$$S_i=\rho\cdot C_d\cdot\alpha_z\cdot\overline{u}_z^2. \quad (7)$$

C_d is the effective drag coefficient, $\overline{u}$ is the wind speed at height z, and α_z is the LAI per unit volume at height z. Following Amiro (1990) C_d was set to 0.15, and a profile of LAI per unit volume was specified as shown in Figure 1. The source term shown in the momentum equation has the following form for a porous media,

$$S_i = -C_2 \cdot \frac{1}{2} \rho \cdot \overline{u}_{mag} \overline{u}_j , \qquad (8)$$

where C_2 is the inertial loss coefficient, given by

$$C_2(z) = 2 \cdot C_d \cdot \alpha_z . \qquad (9)$$

Porous media was also used to represent the trunks of the lodgepole pine canopy. An individual trunk coefficient of drag, C_{d_T}, was found to be 0.9. A coefficient of drag, C_d, representing the entire fetch was calculated by

$$H \cdot L \cdot W \cdot C_d = \sum_i (A_T C_{d_T})_i , \qquad (10)$$

where H, L, W are the height, length, and width of the domain respectively, and A_T is the cross-sectional area of a tree. The coefficient of drag, C_d, was then equated directly to the inertial loss coefficient, C_2,

Solar Radiation

Solar radiation was modeled with a heat source term, S_h. The heat source for a cell with a volume V is calculated as

$$S_h(z) = \frac{dQn(z)}{dz} \cdot V , \qquad (12)$$

with $Qn(z) = Qn(h) \cdot \exp(-aF)$, and the non-dimensional cumulative LAI, F, was calculated as $F = \int_z^h \alpha \, dz$. $Qn(h)$ was fixed at 100 W/m^2 and a, the extinction coefficient, was set to 0.6 following (Shen and Leclerc 1997).

$$C_d = \sum_i (A_T C_{d_T})_i \Big/ H \cdot L \cdot W \quad . \qquad (11)$$

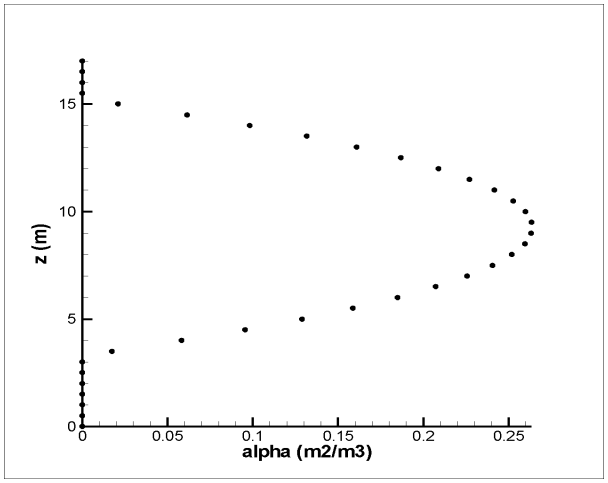

Figure 1: LAI per unit volume (LAI = 2.1)

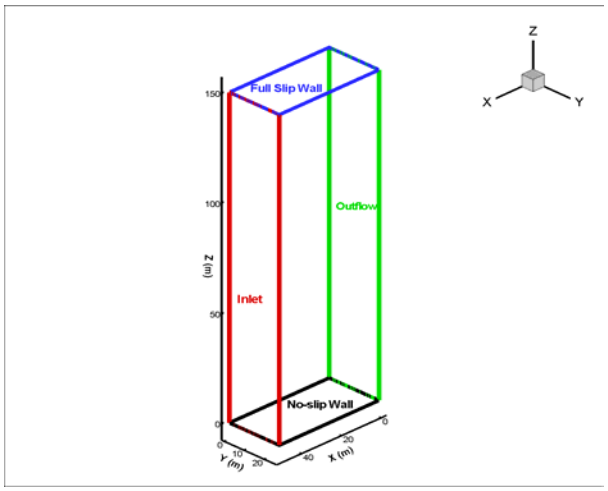

Figure 2: Domain and Boundary Conditions (symmetry boundaries not shown)

Boundary Conditions

A total of 383,000 volume cells were generated in a 50m x 25m x 150m domain shown in figure 2. The source cell had a volume of $0.0125m^2$. Cell size increased from the source cell in all directions shown in Figures 3 and 4.

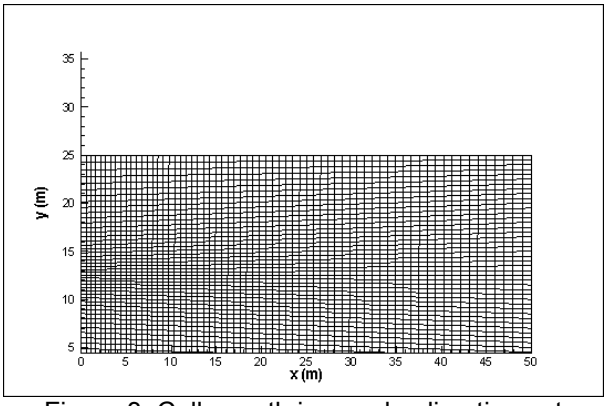

Figure 3: Cell growth in x and y directions at z = 0m.

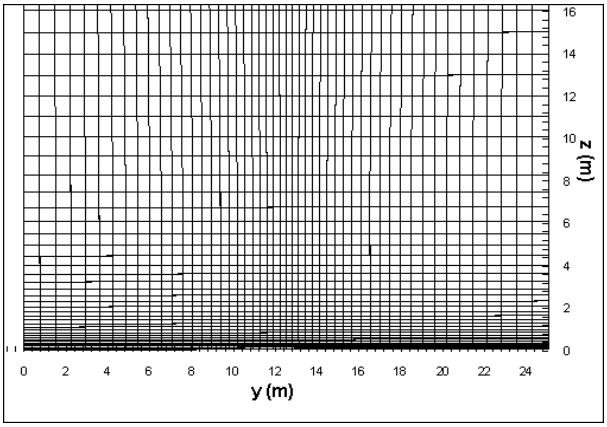

Figure 4: Cell growth in y and z directions at x = 0m.

At the inlet boundary the mean wind, Reynolds stresses, and temperature were specified. A no slip wall boundary represented the ground with a roughness height of 0.3m. A full slip boundary was used at the top wall, symmetry boundaries were specified at the sides of the computational volume. The symmetry boundary condition specifies zero gradients and zero mass flow across the boundary. An outflow boundary condition was specified at the outlet, this boundary condition sets zero stream-wise gradients and also satisfies continuity at every time step by performing a mass balance. The initial inlet profiles of wind speed, turbulent kinetic energy, and dissipation rate were based on approximate profiles from Detering and Etling (1984). After reaching a steady state solution using the k-ε turbulence closure model, new profiles of wind speed and Reynolds stresses were specified at the inlet. The Reynolds stresses were determined using the turbulent kinetic energy and dissipation rate from the k-ε runs. Several runs specifying converged outlet profiles at the inlet boundary, to simulate an infinite fetch, were performed until steady state conditions were reached.

Numerical Methods

The governing equations were discretised using the finite volume method (FVM) with the semi-implicit method used for pressure-linked equation (SIMPLE) algorithm pressure coupling (Patankar 1980). The quadratic upstream interpolation for convective kinetics, QUICK, differencing scheme was used for the momentum, turbulence kinetic energy, turbulence dissipation rate, and the Reynolds stresses. Outlet profiles of velocity and turbulence were imposed on the inlet after each convergence until steady state conditions were reached.

5. RESULTS AND DISCUSSION

Results with and without solar heating using the Boussinesq approximation showed no differences in the velocity and momentum flux profiles. This was due to the small potential temperature gradients. Therefore results for the uniform potential temperature profile are not shown.

Figure 5 illustrates the normalized velocity profile. The height of the canopy, h, is 15m and U is the velocity at this height, 0.22 m/s. A strong wind shear is located at the top of the canopy. Above the canopy the wind follows a logarithmic profile. Another gradient is shown in the canopy below z/h = 0.5. This represents an increase of flow in the under story of the canopy. This profile is similar to velocity profiles found by Raupach and Thom (1981), Amiro (1990), Shen and Leclerc (1997), and Finnigan (2000).

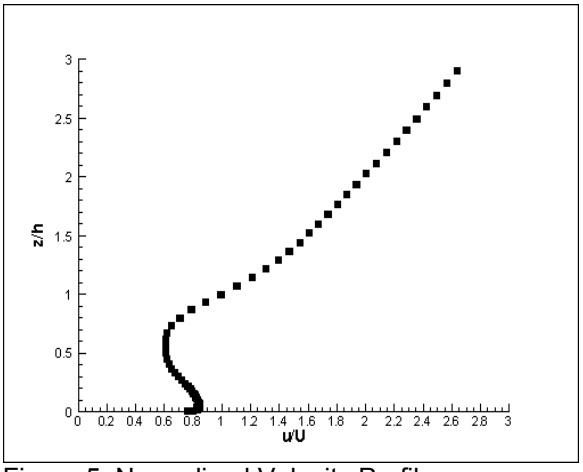

Figure 5: Normalized Velocity Profile.

The vertical Reynolds Stress is shown in Figure 6, and is normalized by u'w'(h) = u* = 0.0128 m^2/s^2 at the top of the canopy.

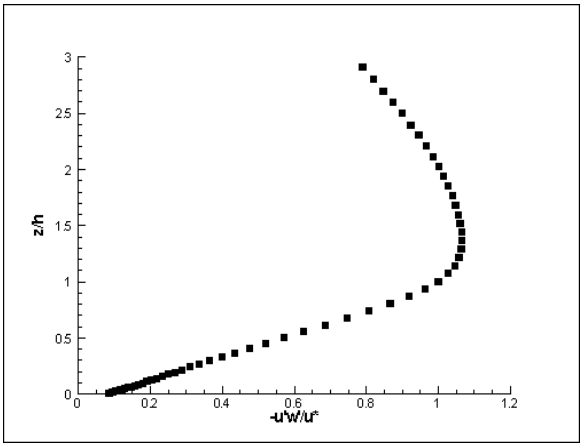

Figure 6: Normalized Vertical Reynolds Stress Profile.

Figure 7 shows the potential temperature profile. The potential temperature decreases with height to the top of the canopy. This represents early morning conditions, where the potential temperature is the highest where the leaf density is the highest (0.8h) and decreases down through the canopy. Above the canopy the potential temperature decreases to a constant value (290 K), then remains that value for the rest of the height of the domain.

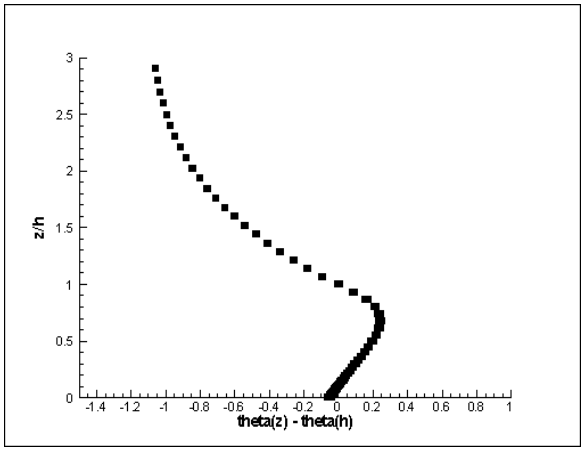

Figure 7: Normalized Temperature Profile.

Lateral and vertical normalized concentration profiles are shown in Figures 8 and 9, respectively. The concentration is normalized by the release rate (Q = 0.00287 kg/m^3-s). The tracer gas source was 1.5m above the ground, and was released from a cell with a volume of $0.0125m^3$. Lateral profiles were taken at a height of 1.5m and at three downstream positions, 5m, 10m, and 30m. Vertical profiles were taken at the same downstream positions, and directly downstream of the source. The profiles show symmetric lateral dispersion as well as maximum concentrations located at the ground. The normalized concentrations (s/m^3) at 1.5m above the ground were 0.20, 0.088, and 0.021 at 5m, 10m, and 30m downstream distances from the source, respectively. The normalized concentrations fall within 95% confidence of median values of maximum normalized concentrations, 0.22, 0.12, and 0.025 at 5m, 10m, and 30m downstream arcs, respectively, reported in Thistle et al. (In Press) for a lodgepole pine canopy. These values were averaged over all sampling periods totaling 81 hours.

6. CONCLUSIONS

A three dimensional steady state numerical computation was used to study dispersion within a generic lodgepole pine canopy. The effective canopy drag was incorporated by porous media. Solar radiation was included as a heat source term with an imposed potential temperature gradient. Normalized velocity, vertical Reynolds stress, and concentration profiles were

reported corresponding to solar heating conditions. The small potential temperature gradient did not affect the flow conditions. Normalized velocity and vertical Reynolds stress profiles agreed with the literature and showed classic features, such as strong shear above the canopy and momentum absorption within the canopy. Normalized concentrations agree with 95% confidence with experimental data over a large averaging period. This agreement suggests that the use of CFD to predict near-field concentrations of a tracer gas within forest canopies is feasible. The next step is to investigate CFD computations for smaller time averages. These computations will require enhanced methods to capture the turbulent dynamics within the forest canopies.

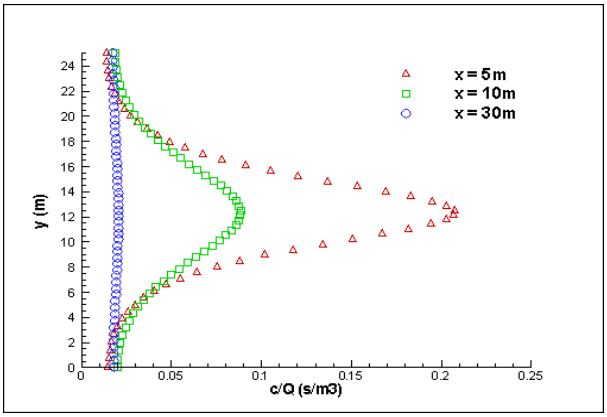

Figure 8: Lateral Normalized Concentration Profiles.

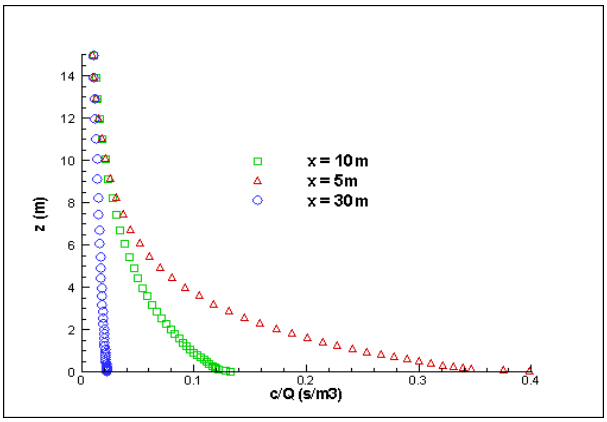

Figure 9: Vertical Normalized Concentration Profiles.

Second order turbulence closure for the momentum equation, and first order closure for the energy and species equations were used. This limits the use of the second order turbulence closure model. To fully capture the turbulent dynamics, the large turbulent eddies should be resolved. Large Eddy Simulation, LES, resolves larger eddies while modeling the smaller dissipating eddies. This study has provided a base from which future work using LES will be conducted.

7. REFERENCES

Amiro, B. D., (1990). “Comparison of Turbulence Statistics within three Boreal Forest Canopies.” Boundary-Layer Meteorology **51**: 99-121.

Amiro, B. D. (1990). "Drag coefficients and turbulence spectra within three boreal forest canopies." Boundary-Layer Meteorology **52**: 227-246.

Arya, S. P. (1999). Air Pollution Meteorology and Dispersion. New York, Oxford University Press.

Detering, H. W. and D. Etling (1984). "Application of the E-e Turbulence Model to the Atmospheric Boundary Layer." Boundary-Layer Meteorology **33**: 113-133.

Finnigan, J. (2000). "Turbulence in Plant Canopies." Annual Review of Fluid Mechanics **32**: 519-571.

Kaimal, J. C. and J. J. Finnigan (1994). Atmospheric Boundary Layer Flows: Their Structure and Measurement. New York, Oxford University Press.

Launder, B. E., G. J. Reece, et al. (1975). "Progress in the Development of a Reynolds-Stress Turbulence Closure." Journal of Fluid Mechanics **68**: 537-566.

Patankar, S. V. (1980). Numerical Heat Transfer and Fluid Flow, McGraw-Hill.

Raupach, M. R. and A. S. Thom (1981). "Turbulence in and Above Plant Canopies." Annual Review of Fluid Mechanics **13**: 97-129.

Shen, S. and M. Y. Leclerc (1997). "Modelling the turbulence structure in the canopy layer." Agriculture and Forest Meteorology **87**: 3-25.

Thistle, H. W., H. Peterson, et al. (In Press). "Surrogate Pheromone Plumes in Three Forest Trunk Spaces: Composite Statistics and Case Studies."

U.S.D.A. Forest Service (2003). America's Forests Health Update. Washington, D.C., U.S.D.A. Forest Service, Forest Health Protection: 14,15.